ELSEVIER

Journal of Marine Systems 37 (2002) 129–149

JOURNAL OF MARINE SYSTEMS

www.elsevier.com/locate/jmarsys

# Summer and winter surveys of the Subtropical Front of the southeastern Indian Ocean 1997–1998

Charles James[a,*], Matthias Tomczak[a], Ian Helmond[b], Lindsay Pender[b]

[a] *Flinders Institute for Atmospheric and Marine Sciences, The Flinders University of South Australia, FIAMS GPO Box 2100, Adelaide, SA 5001, Australia*

[b] *CSIRO Division of Marine Research, GPO Box 1538, Hobart, TAS 7001, Australia*

Received 25 November 2000; received in revised form 15 April 2002; accepted 20 April 2002

**Abstract**

The Subtropical Front (STF) in the region south of Australia was surveyed to determine its location, character, and seasonal variation. The survey consisted of two cruises, during summer and winter of 1998, and used a towed CTD system (SeaSoar).

Based on observations, the STF does not appear to be continuous between the Indian and Pacific Oceans in the region south of Tasmania during winter; instead, it appears to end at the continental shelf of western Bass Strait near 40°S.

During both seasons, the STF is characterized by moderate to strong density compensation with the horizontal density ratio ($R_\rho = \alpha\Delta T/\beta\Delta S$) close to 1 both in and below the mixed layer. This contrasts with observations in other regions where $R_\rho$ tends towards 2 below the mixed layer. We observed a high degree of interleaving, submerged eddies and small scale temperature and salinity variability. This is attributed to the interaction of a front that is density compensated with a local wind field that periodically reverses direction.



*Keywords:* Subtropical Front; Summer; Winter; Density compensation; SeaSoar; Australia, 119–147°E, 36–45°S

## 1. Introduction

Between the core of the Trade Winds and the maximum Westerlies, which stretch around the globe between approximately 20° and 45° on either side of the equator, is a region characterized by negative wind stress curl in the atmosphere and by associated Ekman transport convergence in the ocean. In oceanography this region has become known as the Subtropical Convergence Zone (SCZ). This region is also characterized by a decrease of sea surface temperature (SST) from the tropics to the temperate zones, accompanied by a decrease of sea surface salinity (SSS). As a general rule, the poleward increase of surface density produced by the decrease in SST is larger than the compensating decrease of surface density produced by the decrease in SSS, and as a consequence surface density tends to increase with distance from the equator.

Embedded within the SCZ and somewhat on its poleward side is a zonal band of enhanced meridional SST and SSS gradients known as the Subtropical Front

* Corresponding author. Tel.: +61-8-201-2724; fax: +61-8-201-2676.

*E-mail address:* Charles.James@flinders.edu.au (C. James).

0924-7963/02/$ - see front matter. 
PII: S0924-7963(02)00199-9

(STF). In the southern hemisphere this front extends from the coast of Argentina, where it is found near 30°S, through the Atlantic, shifting gradually southward to 40°S south of Africa and continuing along that latitude through the Indian and central Pacific Oceans, where it shifts northward again to arrive at the coast of Chile as far north as 25°S (Tomczak and Godfrey, 1994). The STF defines the southern limit of the subtropical gyres, separating them from the broad westward flow of the Circumpolar Current which lies further south (Stramma and Peterson, 1990; Stramma, 1992; Stramma et al., 1995).

Compared with other frontal systems of the world ocean, the STF is relatively weak, displaying a temperature contrast of about 2 °C and a salinity contrast of about 0.5 ‰ over a frontal zone distance of 200 km. In addition, the STF is located in a region of large short-term and seasonal variability with a high incidence of eddy formation and eddy shedding. This means that although on synoptic scales the STF is a very distinct feature of the subtropics, where it can be seen to at least 250 m depth during meridional crossings, the STF is rarely observed in atlas data of ocean climate based on long-term averages of property distributions.

One of the features of the STF south of Australia is that it is a density compensated front both above and below the surface mixed layer. Density compensation in the mixed layer is not a unique phenomenon and has been reported for the North Pacific (Rudnick and Ferrari, 1999) and for the Southern Ocean between Tasmania and Antarctica (Rintoul and Bullister, 1999; Rintoul et al., 1997). Compensation below the mixed layer, however, appears to be a more unusual phenomenon with observations indicating that below the mixed layer, temperature gradients generally dominate the density structure by a factor of two (Schmitt, 1999). In our study, we found the temperature influence below the mixed layer relatively small and the density structure quite strongly compensated.

Stramma (1992) shows that east of South Africa the STF is associated with a geostrophic transport of some 30 Sv (1 Sv = $10^6$ $m^3$ $s^{-1}$) and that this transport is reduced to 10 Sv as Australia is approached. South of Australia it decreases further, reaching negligible magnitude east of 130°E (Schodlok et al., 1997; Schodlok and Tomczak, 1997). Belkin and Gordon (1996) also report that the interaction between the STF and the Subantarctic Front (SAF) in the central Southern Indian Ocean appears to strengthen the SAF at the expense of the STF. These observations are consistent with strong compensation where the effects of the temperature and salinity changes across the STF result in little or no density gradient and where this compensation extends below the mixed layer. This raises the question of whether the general STF really is a continuous feature between the Indian and Pacific Oceans as it is commonly described (Belkin and Gordon, 1996).

This paper details observations taken during two research voyages in 1998. The voyages were designed to investigate the structure and continuity of the STF during summer and winter conditions. Although the first cruise was the summer cruise, we will address winter observations first since the winter observations are less complicated and therefore easier to interpret.

## 2. Data and methods

The data describing the STF were collected by R/V *Franklin* during the austral summer (voyage FR02/98, from 30 January to 17 February, 1998) and winter (voyage FR10/98, from 30 July to 18 August, 1998). Both surveys cover the region south of Australia from 118°E to Tasmania. Figs. 1 and 2 show average SST during each research voyage as seen by satellite. Similar information was available before the voyages and was used to guide the ship along the tracks shown in the figures. The voyages were designed to achieve as many crossings of the STF as possible within the available time span. The locations of individual crossings were based on satellite SST information available before the cruises and updated as new SST images became available during the voyages.

The front was surveyed with a SeaSoar towed CTD system and an acoustic Doppler current profiler (ADCP). The SeaSoar is a remotely controlled device fitted with a dual CTD system which is towed behind the ship at a speed of 8 knots (1 knot = 1.852 km/h) and undulates over a depth range of up to 300 m. For the winter investigation the flight path was set to cover the depth range 10–300 m, which gives a repetition rate between successive dives of about 4 min or a distance between dives of 1.2 km. The mixed layer during summer is much shallower than during winter, consequently the SeaSoar profiling range was only 10–200 m. The shallower range during the summer

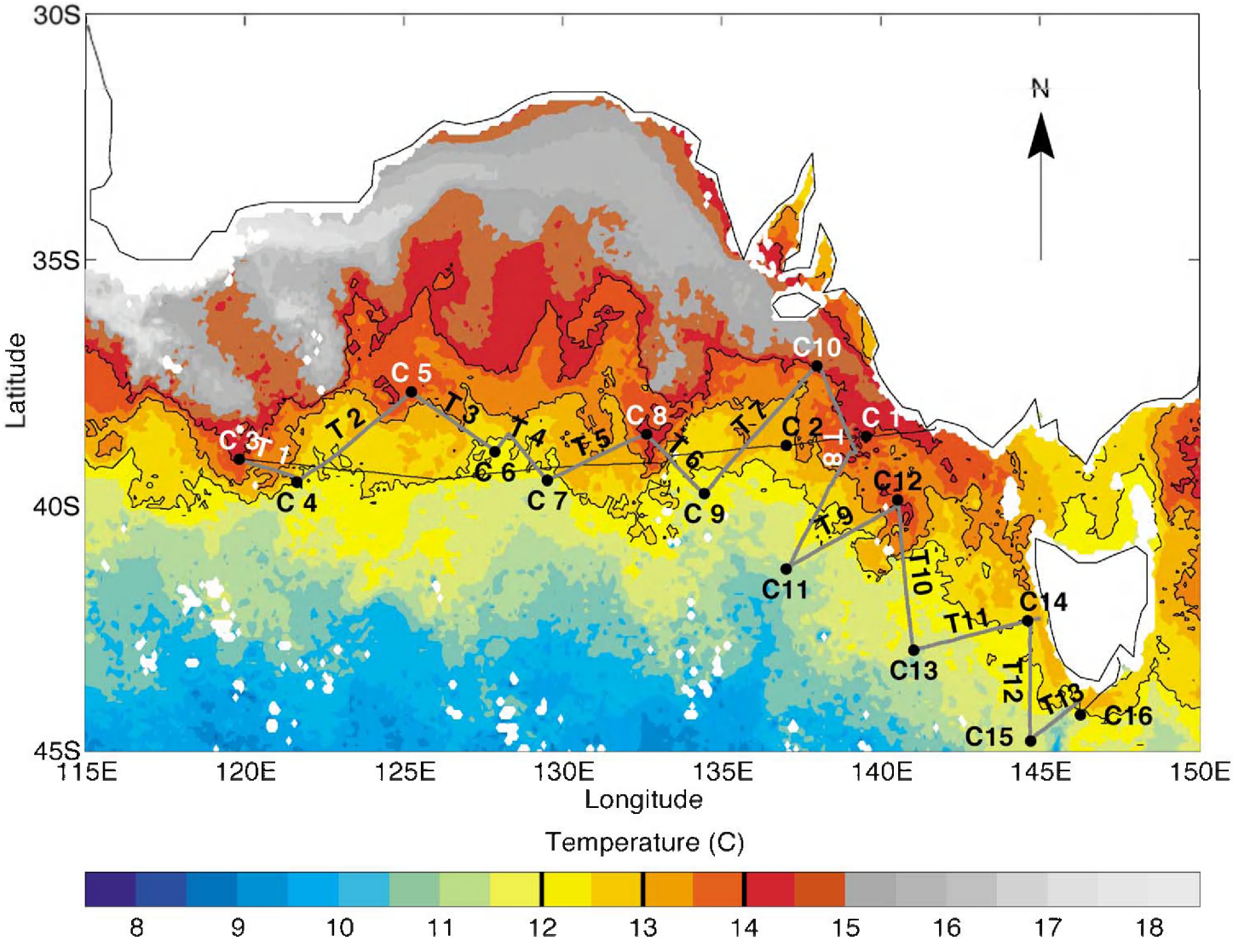


Fig. 1. The cruise track of R/V *Franklin* voyage FR 10/98 superimposed on the mean SST for the period 30 July–19 August, 1998 as derived from all available satellite SST images for that period. CTD stations are labeled C1–C11 and marked as dots; individual transects are labeled T1–T11 and highlighted. The 12, 13 and 14 °C isotherms are highlighted in the image and in the color legend.

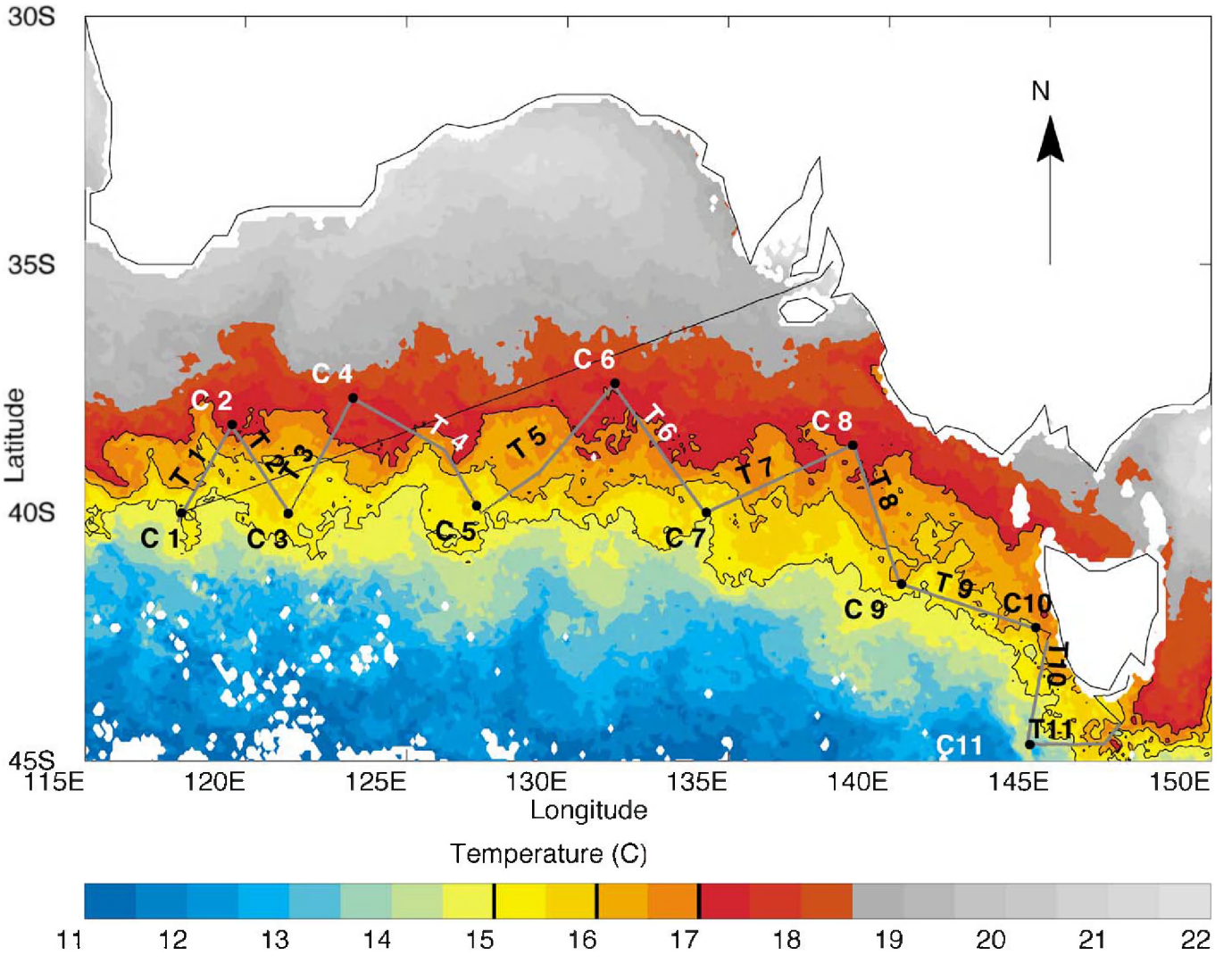


Fig. 2. The cruise track of R/V *Franklin* voyage FR 02/98 superimposed on the mean SST for the period 30 January–20 February, 1998 as derived from all available satellite SST images for that period. CTD stations are labeled C1–C16 and marked as dots; individual transects are labeled T1–T13 and highlighted. The 15, 16 and 17 °C isotherms are highlighted in the image and in the color legend.

resulted in a shorter duration of each dive (about 2.5 min), and consequently a horizontal distance between successive dives of about 1 km.

In addition to SST, the satellite images (Figs. 1 and 2) show the location of CTD stations and the names of numbered transects. CTD profiles to 1500 m were taken at the beginning and end of every transect except at the end of the last transect of the summer cruise (T11). The CTDs were used to make estimates of geostrophic transport as well as to calibrate the SeaSoar. During the winter cruise two CTD profiles were taken prior to reaching the start of the first transect, these profiles were performed to take advantage of a fortuitous front crossing near the beginning of the voyage. One consequence of this is that transect numbers lag CTD numbers by 2 stations. Additional CTD profiles to 250 m depth were performed at 10 nautical mile intervals (1 nautical mile = 1.852 km) on the few occasions during the summer cruise when problems with the SeaSoar resulted in significant data gaps.

An unexpected problem not encountered on other SeaSoar voyages in the tropics and temperate regions was the occasional malfunctioning of the conductivity sensors due to clogging from jellyfish, salps, or other marine life. This was presumably due to the high density of marine life in the STF. The obstruction of the conductivity cell usually cleared itself within a few minutes. Because the SeaSoar was equipped with a dual CTD system, on most occasions only one of the two conductivity cells was affected by clogging; a careful investigation of the temperature–salinity diagrams of both CTD systems led to the elimination of most, but not all, erroneous data points. As a result of this experience the conductivity cells were fitted with deflectors during the winter voyage, and the problem did not reoccur.

The SeaSoar was recovered between front crossings and calibrated by placing the dual CTD system into a seawater bath. Additional calibration checks were made against CTD data.

The raw SeaSoar data were averaged to 2 m depth increments and converted, by interpolation, into vertical CTD-type casts with a variable horizontal resolution ( ~ 1.5 km). Data from CTD stations were likewise subsampled to 2 m depth increments. The SeaSoar profiles presented in this paper were additionally horizontally interpolated to a constant along-track resolution of 1.1 km for the summer and 1.3 km for the winter. Significant data gaps were left blank.

Temperature and salinity gradient criteria were used to identify the location of the STF. Previous investigators used various definitions to define the STF; Belkin and Gordon (1996) list 15 different criteria used by investigators between 1933 and 1995. Most of the early definitions were aimed at defining the STF for the entire southern hemisphere and are therefore quite broad (Deacon, 1960, for example, uses the SST range 8–12 °C for winter and 12–16 °C for summer to define the STF). More recent definitions place the STF at the location where the 12 °C isotherm crosses the 150-m (Nagata et al., 1988) or the 200-m (Orsi et al., 1993) depth level. We found that the existence of the 12 °C isotherm at 150 m ($T_{12}$) was an acceptable predictor of the front location below the mixed layer for both cruises, although the front location in the mixed layer was sometimes offset from the deeper front, especially during the summer cruise.

At this point, it is worth elaborating on the terminology we have chosen to describe the degree of density compensation. In a density compensated front like the STF, the gradients of temperature and salinity have the same sign (if the gradients of temperature and salinity have the opposite sign then the density gradient is enhanced rather than compensated). This results in a density gradient less than that which would have been produced by the temperature or salinity gradient alone. In this paper we frequently refer to a frontal section as being strongly or weakly compensated. Strong compensation occurs when the temperature and salinity gradients combine to produce near zero density gradient, and weak compensation occurs when the temperature and salinity gradients, while still having the same sign, combine to produce a significant density gradient. A more objective way to compare the degree of density compensation is to use a modification of the Turner angle commonly used in double-diffusive studies (SCOR Working Group 69, 1988). Our modified Turner angle is the arctangent of the density ratio ($R_\rho = \alpha\Delta T/\beta\Delta S$) given by $T_H = \mathrm{atan}(\alpha\Delta T/\beta\Delta S)$, where $\Delta T$ and $\Delta S$ are paired temperature and salinity changes in a horizontal rather than a vertical direction, $\alpha = (1/\rho)(\Delta\rho/\Delta T)$ (the thermal expansion coefficient), and $\beta = (1/\rho)(\Delta\rho/\Delta S)$ (the haline contraction coefficient). Complete density compensation is indicated by a modified Turner angle of 45°,

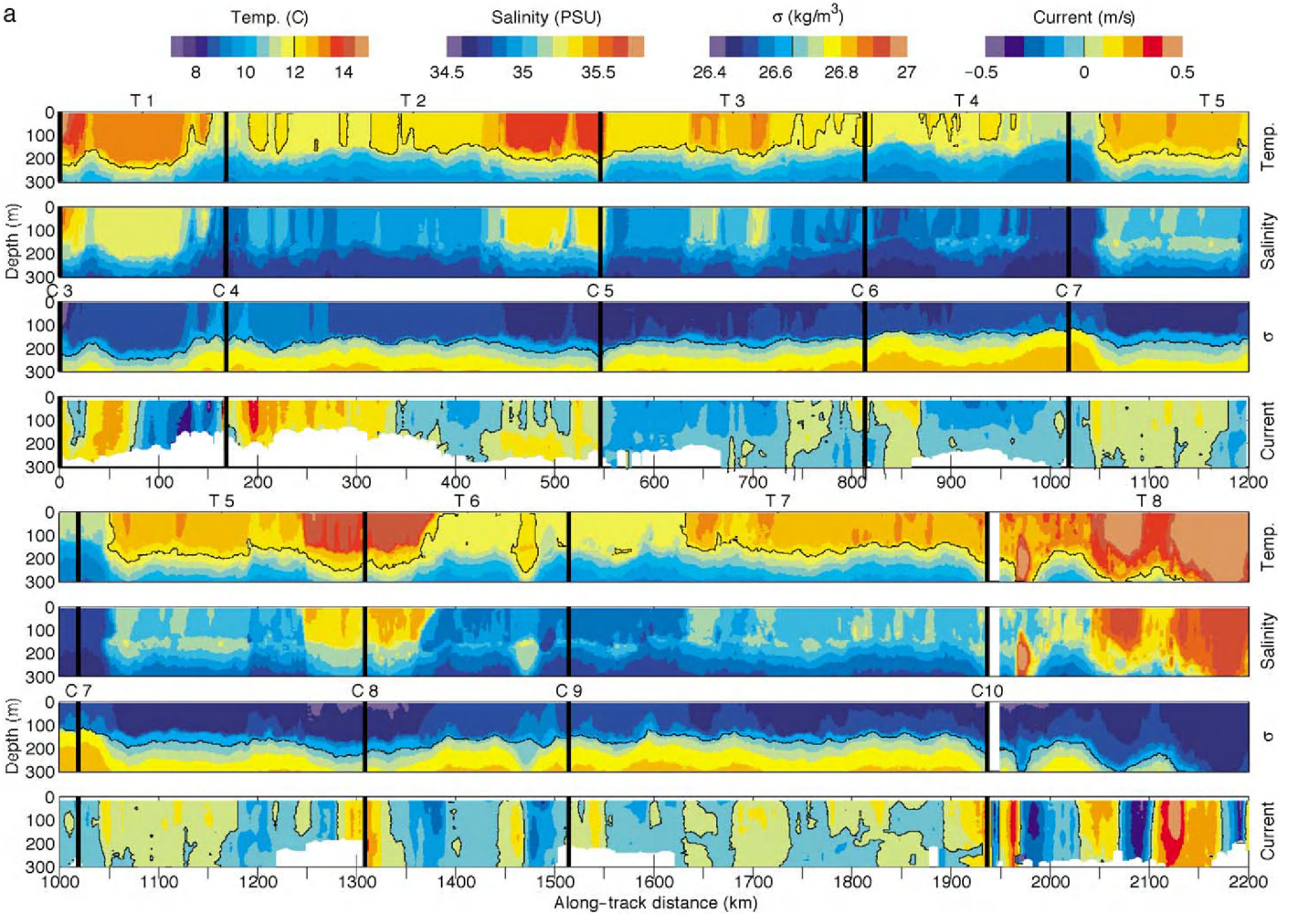


Fig. 3. (a,b) Temperature (°C), salinity (‰), and density ($\sigma$) from Seasoar data and velocity (m/s) from ADCP record for the winter cruise, FR 10/98. Black vertical bars indicate CTD stations. The 12 °C isotherm, the 26.65$\sigma_t$ isopycnal, and the 0 m/s contour are highlighted in the profile and in the color legends. ADCP velocities are measured perpendicular to the ship's track with positive velocities to the right of the ship's course.

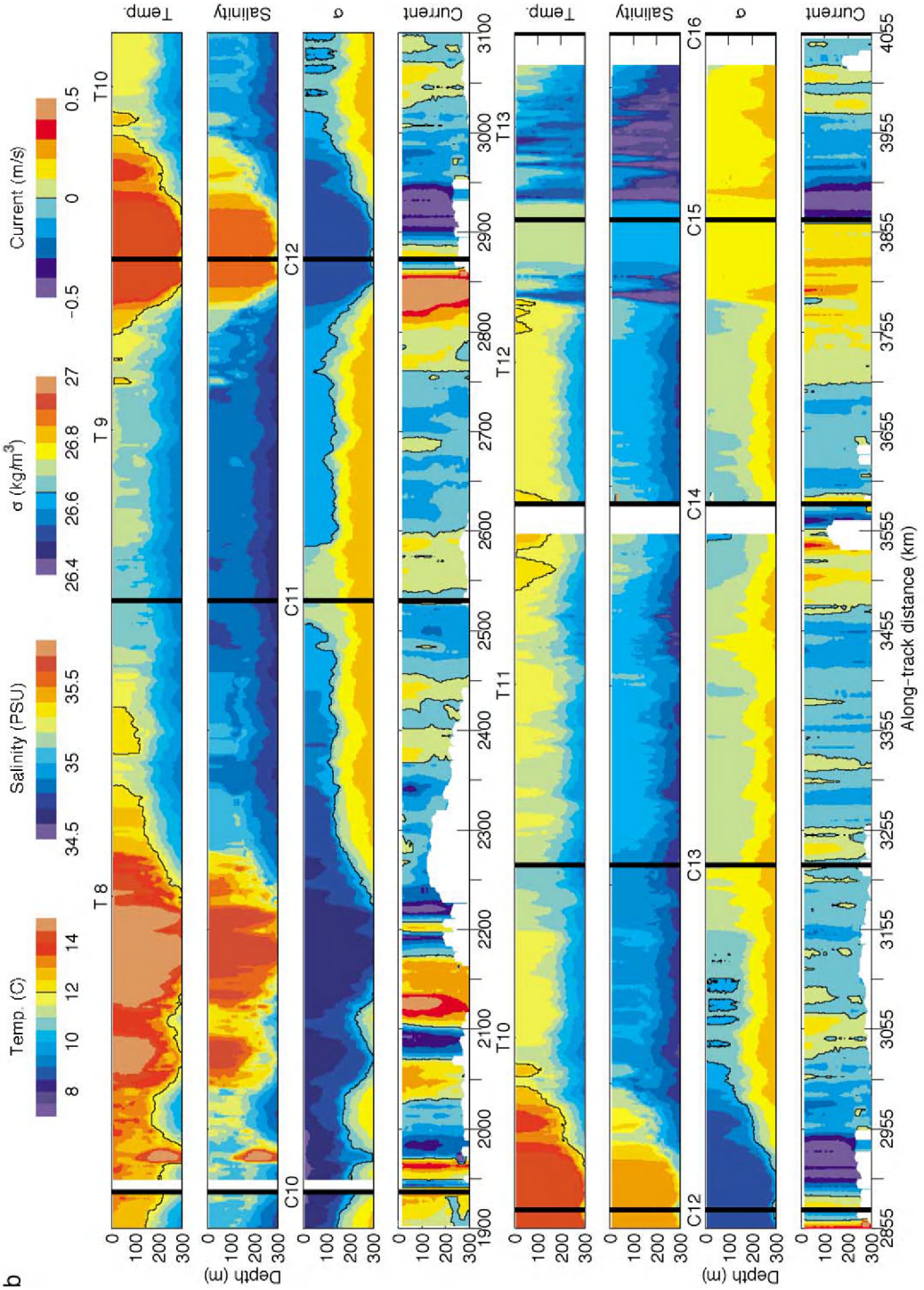


Fig. 3 (*continued*).

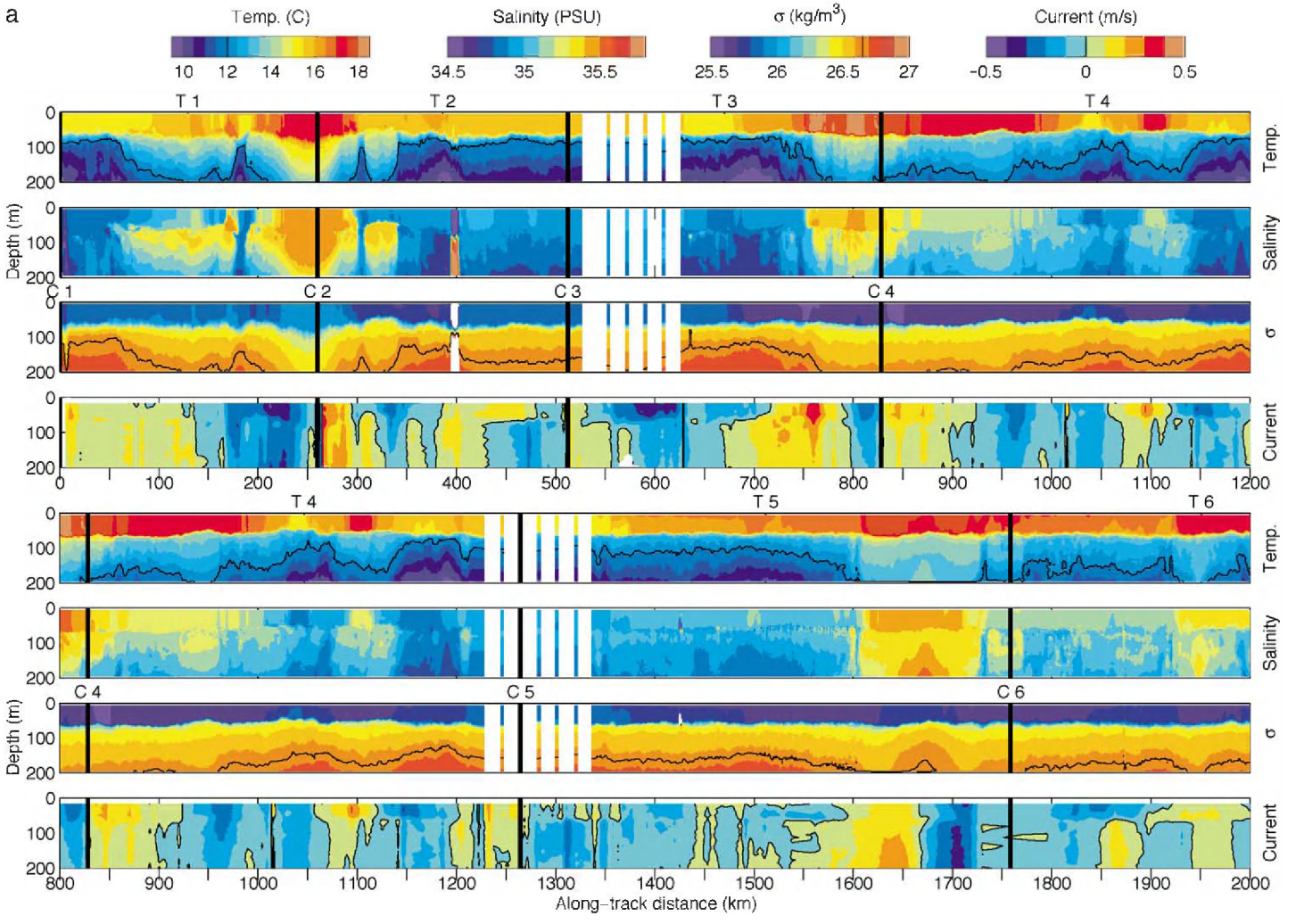


Fig. 4. (a,b) Temperature (°C), salinity (‰), and density ($\sigma$) from Seasoar data and velocity (m/s) from ADCP record for the summer cruise, FR 02/98. Black vertical bars indicate CTD stations. The 12 °C isotherm, the 26.65$\sigma_t$ isopycnal, and the 0 m/s contour are highlighted in the profile and in the color legends. ADCP velocities are measured perpendicular to the ship's track with positive velocities to the right of the ship's course.

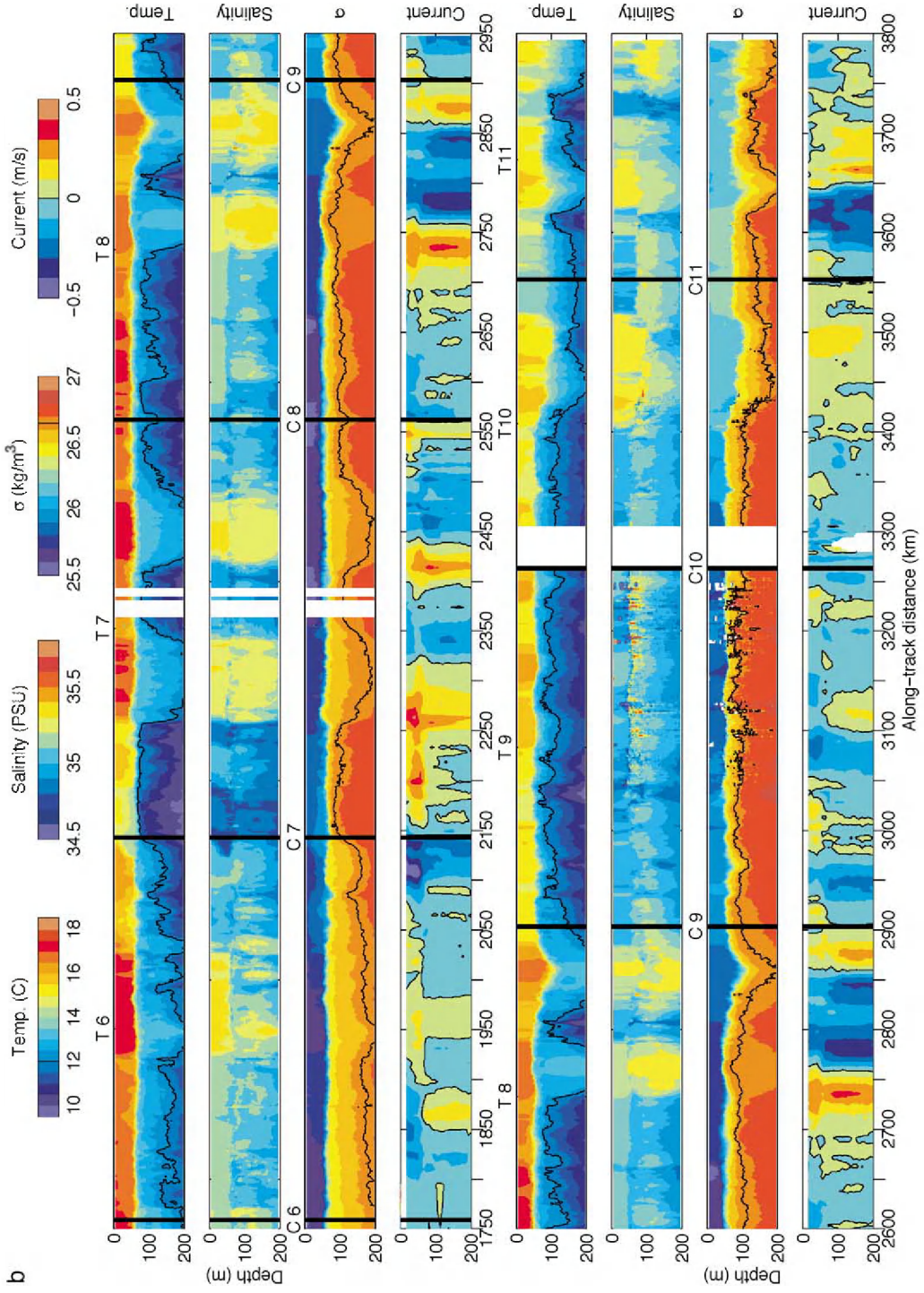


Fig. 4 (*continued*).

where the density ratio is equal to unity. One advantage of using $T_H$ instead of $R_\rho$ is that it gives equal weight to changes in temperature and in salinity; $R_\rho$ is particularly sensitive to small changes in S.

$T_H$ was calculated for each transect by linear regression of $\alpha\Delta T$ and $\beta\Delta S$. Four severe spikes in the summer salinity record were removed prior to processing. The first spike occurred between 0 and 12 km, the second spike was between 392 and 404 km, the third spike was between 1423 and 1474 km, and the last spike was between 3187 and 3191 km. Other smaller amplitude, high-frequency anomalies between summer C9 and C11 were not removed as they were far too numerous; they did, however, contribute to an increase in the error of the regressions. The error in $T_H$ was estimated by taking the difference between $T_H$ calculated by a regression of $\alpha\Delta T$ vs. $\beta\Delta S$ and $T_H$ calculated by a regression of $\beta\Delta S$ vs. $\alpha\Delta T$.

## 3. Results

The observations from the winter and summer cruises are shown in Figs. 3–8. Figs. 3 and 4 show the full SeaSoar tracks for each cruise. Figs. 5 and 6 show the winter and summer geostrophic transports relative to 1480 dbar calculated from the CTDs taken at the beginning and end of each transect (with the exception of T11 from the summer cruise). Figs. 7 and 8 show the modified Turner angle within the mixed layer and below the mixed layer for the winter and summer. Table 1 summarizes the geostrophic transports and the Turner angles for all transects from both cruises. Table 2 lists the significant front crossings based on the $T_{12}$ criterion and includes notes about various features discussed in the text.

For the remainder of this section, we draw the reader's attention to a number of interesting features visible in the SeaSoar and ADCP profiles.

### 3.1. Winter

The first two transects lie at the western limit of the STF south of Australia. Here we find strong gradients in temperature, salinity and density as well as moderate ADCP velocities. The ADCP velocities may reflect geostrophic transport associated with the density gradient. Starting at km 200, the density profile shows

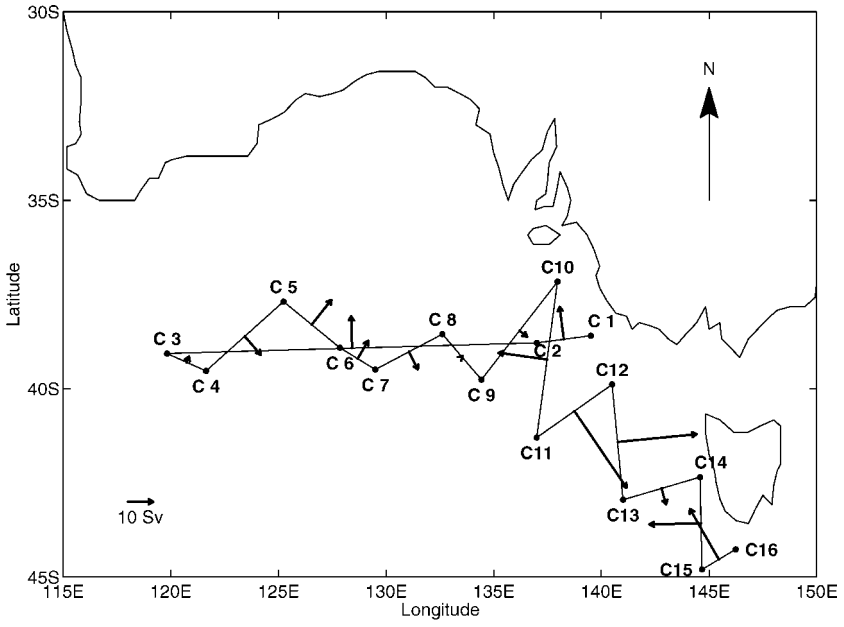


Fig. 5. Geostrophic transport (Sv) measured between consecutive CTD stations during the winter cruise, FR 10/98. CTD stations are labeled C1–C11 and marked. Note, straight lines between CTDs for geostrophic calculations do not necessarily align with transects.

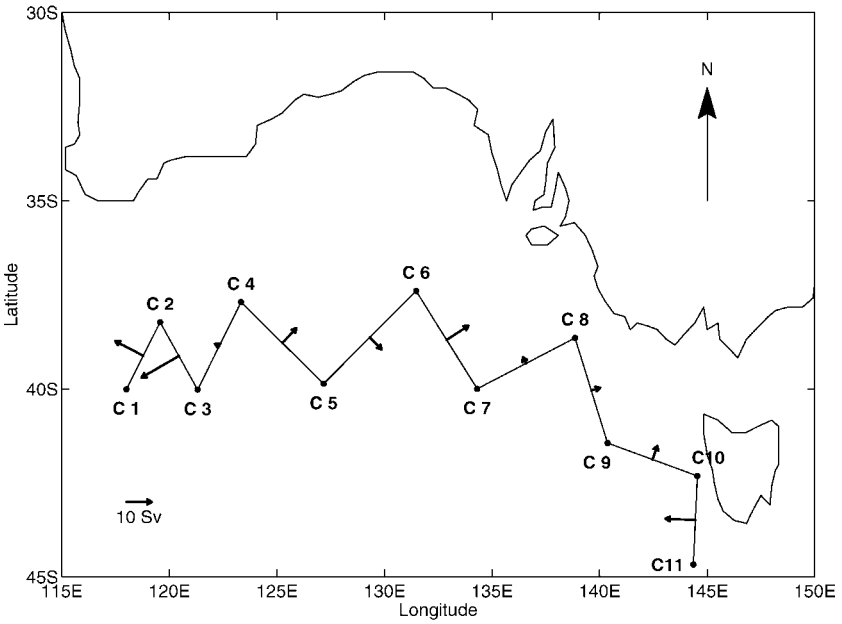


Fig. 6. Geostrophic transport (Sv) measured between consecutive CTD stations during the summer cruise, FR 02/98. CTD stations are labeled C1–C16 and marked. Note, straight lines between CTDs for geostrophic calculations do not necessarily align with transects.

very little variation for nearly 1800 km despite crossing the STF at least five times. ADCP measured currents are weak and probably dominated by tidal currents.

The first significant change in the density structure occurs near the beginning of T8 at km 1970 where an isolated sub-surface feature below 100 m is associated with high temperature and salinity as well as strong horizontal shear in the ADCP velocities. One possible source for this feature is the high salinity water from Spencer Gulf or the Gulf of St. Vincent. Pulses of this water have been periodically observed at the continental shelf break (Lennon et al., 1987). T8 is the longest transect and starts out following the continental shelf before moving slowly into oceanic depths.

Although T8 begins on the warm side of the STF, as we head south, we enter a region of even warmer and higher salinity water. The satellite SST data (Fig. 1) shows that the STF is very filamented in this region and that the warmer water is not formed locally but advected from the west. The high salinity excludes the Leeuwin Current as its source so the water was probably formed in the central Great Australian Bight (Herzfeld, 1997).

For the next 400 km (up to km 2293), the density remains quite low and the mixed layer descends below the 300 m vertical range of the SeaSoar between km 2140 and 2240. The front here is associated with strong ADCP currents that appear to be geostrophically balanced with respect to the density gradient. One interesting feature here is the salinity inversion which is continuous between km 2370 and 2450 at 150 m, this is also associated with a temperature inversion at the same depth which is visible in the SeaSoar profile at km 2400.

We cross to the warm side of the STF for the final time at the end of T9 at km 2824, the strong density gradient here is again associated with strong ADCP currents. As would be expected, density compensation is weaker in both layers. T10 runs nearly north–south and we leave the warm water for the last time at km 2978. South of this point we never again find a front with the temperature characteristics of the STF. This is despite towing the SeaSoar as close to Tasmania as we could during T11.

For the next 800 km we find moderate density compensation in the mixed layer, which appears to be about 200 m deep here. Below the mixed layer,

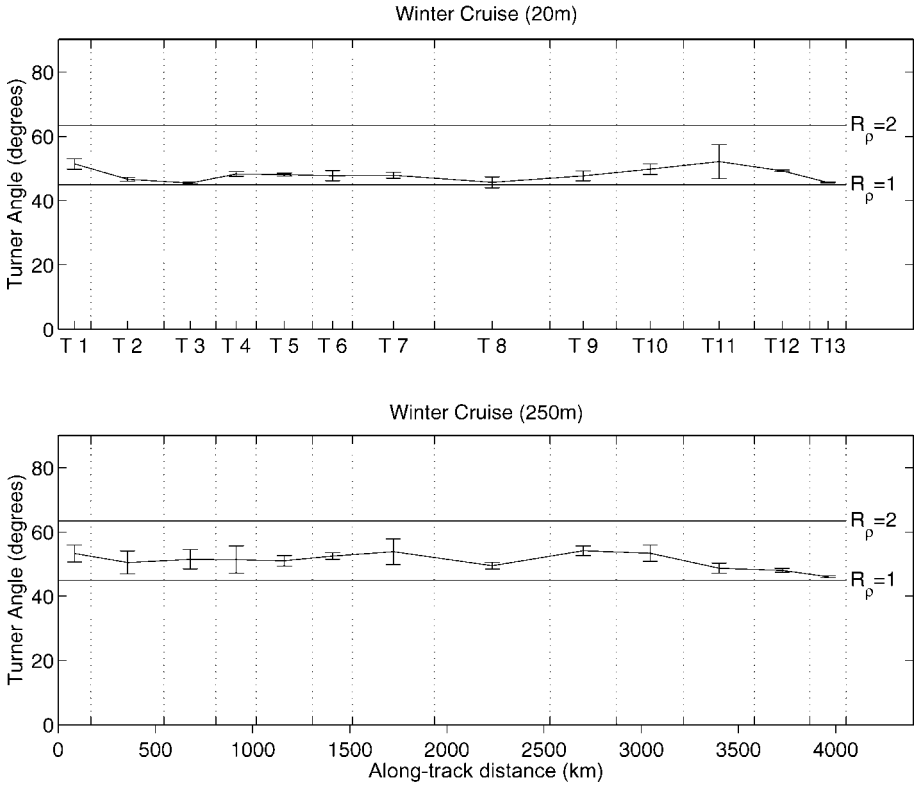


Fig. 7. The modified Turner angle (see text) for the winter cruise, FR 10/98, in the mixed layer at 20 m (top) and below the mixed layer at 250 m (bottom) along the ship's track. Vertical bars indicate error estimate described in the text. Perfect density compensation is indicated by an angle of 45°.

however, density compensation is actually increasing for the remainder of the cruise. Near the end of T12 we find an intense front at km 3785 but although it is not density compensated it is only associated with moderate ADCP currents. The temperature drops from 12 °C to less than 9 °C. We do not believe that this is an expression of the STF, however, since there is no evidence to suggest that we have crossed back onto the warm side of the STF since the last conclusive occurrence of the STF at the start of T10.

As the transect continues south, the temperature and salinity both recover but this time the density is perfectly compensated and this remains the case for the remainder of the cruise. The final transect, T13, returns to the cold water, but despite a few warmer intrusions above 200 m there is no evidence of a coherent front. The mixed layer appears to be deeper than 300 m and consequently the density compensation at both 20 and 250 m are almost the same and close to complete ($T_H$=45.63° and 46.11°, respectively).

### 3.2. Summer

During the summer cruise it was difficult to track the STF due to the shallow ( ~ 50 m) mixed layer which prevents the surface expression of the characteristic 12 °C isotherm. Instead, the cruise track was determined on the basis of SST gradient calculated using the real time data from the ship's thermosalinograph; the largest gradients were generally found between 15 and 18 °C. As during the winter cruise, SST gradients were particularly strong in the western part of the survey region where the Leeuwin Current reaches its southernmost extent (Fig. 2) advecting warm subtropical water.

The first two summer transects show a couple of important features. The surface mixed layer caps two

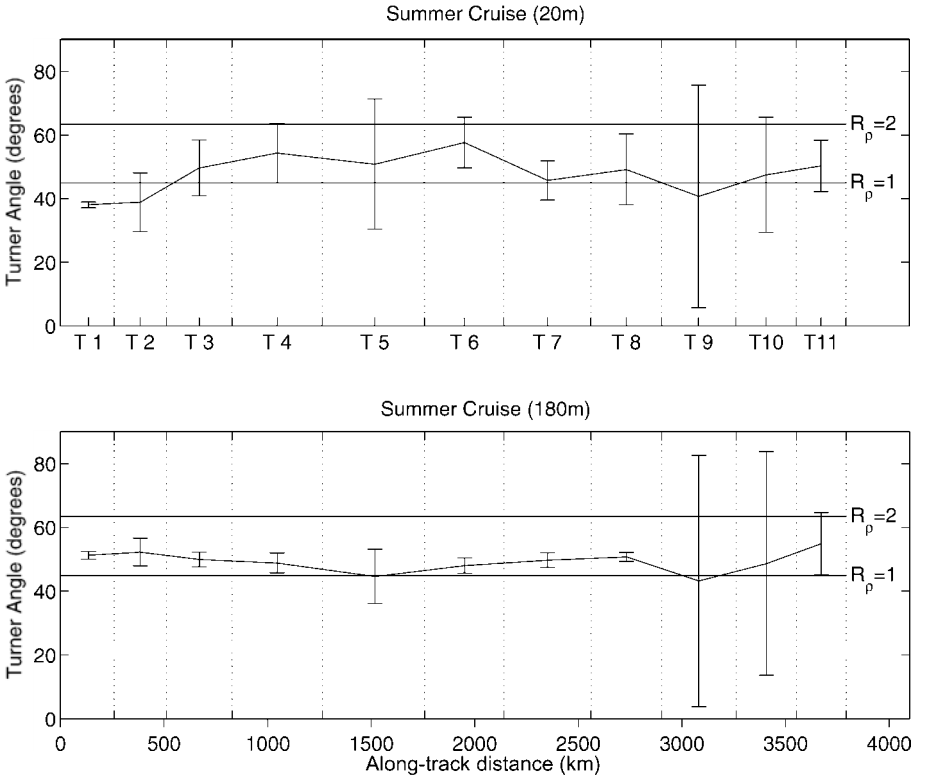


Fig. 8. The modified Turner angle (see text) for the summer cruise, FR 02/98, in the mixed layer at 20 m (top) and below the mixed layer at 180 m (bottom) along the ship's track. Vertical bars indicate error estimate described in the text. Perfect density compensation is indicated by an angle of 45°.

subsurface salinity anomalies; one at km 89–175 and another at km 309–340. The two features may be connected as we have turned a corner at C2 to head south again, but this cannot be confirmed from the SeaSoar observations since the two features are separated by about 125 km in space. The salinity structure is not capped between km 200 and 300 so the salinity expression of the STF does extend to the surface here. The density structure is not compensated at C2 and the 12 °C isotherm follows the $26.65\sigma_t$ isopycnal quite closely. Again, this is similar to the winter situation. Both the ADCP (Fig. 4a) and the geostrophic transports (Fig. 6) show strong westward flow and the satellite image (Fig. 2) indicates that C2 is in a filament or eddy being shed from the STF. The direction of the flow appears to be governed by dynamics below the 200 m range of the SeaSoar. Fig. 9 shows the first 3 corner CTD casts which extend down to 1500 m. Below 400 m the temperature and salinity tendency is actually reversed and the cooler, fresher water is located on the warm side of the front. This gives rise to a *westward* geostrophic velocity relative to 1480 m that reaches a local maximum 420 m below the surface. A large spike in the salinity between km 392 and 404 appears to be due to biological interference with the conductivity sensor.

The beginning of the T3 was marred by instrument problems, shallow CTD casts were used to help fill in the overall profile, but the lack of horizontal resolution limits the usefulness of observations in this region. We were, however, able to confirm that we were still on the cool side of the front until km 761. The front is moderately density compensated with $T_H$ in both layers near 50°. The structure below the mixed layer on the warm side of the front is quite strongly compensated in the horizontal. The columns of uniform salinity and temperature between km 761 and 820 are not reflected in the density field. The structure itself suggests recent

Table 1
Summary of modified Turner angle (see text) within the mixed layer and below the mixed layer and geostrophic transport for both winter and summer voyages

| Season | Transect | Within mixed layer | | | Below mixed layer | | | Geostrophic transport (Sv) |
|---|---|---|---|---|---|---|---|---|
| | | Turner angle (degrees) | Regression error (degrees) | Density ratio | Turner angle (degrees) | Regression error (degrees) | Density ratio | |
| Winter | T1 | 51.45 | 1.64 | 1.25 | 53.33 | 2.63 | 1.34 | 2.21 |
| | T2 | 46.66 | 0.61 | 1.06 | 50.54 | 3.55 | 1.21 | 9.47 |
| | T3 | 45.50 | 0.40 | 1.02 | 51.53 | 3.05 | 1.26 | 12.33 |
| | T4 | 48.30 | 0.71 | 1.12 | 51.42 | 4.25 | 1.25 | 7.92 |
| | T5 | 48.14 | 0.46 | 1.12 | 51.09 | 1.70 | 1.24 | 7.47 |
| | T6 | 47.77 | 1.59 | 1.10 | 52.54 | 1.08 | 1.31 | 0.17 |
| | T7 | 47.92 | 0.97 | 1.11 | 53.90 | 3.96 | 1.37 | 3.79 |
| | T8 | 45.70 | 1.70 | 1.02 | 49.53 | 1.03 | 1.17 | 19.79 |
| | T9 | 47.73 | 1.55 | 1.10 | 54.22 | 1.49 | 1.39 | 36.55 |
| | T10 | 49.81 | 1.67 | 1.18 | 53.42 | 2.51 | 1.35 | 32.01 |
| | T11 | 52.14 | 5.26 | 1.29 | 48.75 | 1.56 | 1.14 | 6.24 |
| | T12 | 49.27 | 0.26 | 1.16 | 48.11 | 0.65 | 1.11 | 20.70 |
| | T13 | 45.63 | 0.08 | 1.02 | 46.11 | 0.31 | 1.04 | 22.72 |
| Summer | T1 | 38.08 | 0.88 | 0.78 | 51.32 | 1.24 | 1.25 | 12.50 |
| | T2 | 38.88 | 9.27 | 0.81 | 52.28 | 4.29 | 1.29 | 17.02 |
| | T3 | 49.65 | 8.78 | 1.18 | 50.01 | 2.30 | 1.19 | 1.61 |
| | T4 | 54.35 | 9.31 | 1.39 | 48.87 | 3.09 | 1.15 | 7.86 |
| | T5 | 50.85 | 20.47 | 1.23 | 44.67 | 8.50 | 0.99 | 6.47 |
| | T6 | 57.63 | 7.95 | 1.58 | 48.07 | 2.39 | 1.11 | 10.21 |
| | T7 | 45.77 | 6.20 | 1.03 | 49.79 | 2.30 | 1.18 | 2.48 |
| | T8 | 49.18 | 11.21 | 1.16 | 50.81 | 1.39 | 1.23 | 3.46 |
| | T9 | 40.74 | 34.96 | 0.86 | 43.24 | 39.32 | 0.94 | 5.41 |
| | T10 | 47.51 | 18.08 | 1.09 | 48.69 | 35.05 | 1.14 | 11.92 |
| | T11 | 50.35 | 8.07 | 1.21 | 54.93 | 9.68 | 1.42 | N/A |

Turner angle and density ratios within the mixed layer are measured at 20 m for both seasons; Turner angle and density ratios below the mixed layer are measured at 250 m for the winter cruise and 180 m for the summer cruise. Geostrophic transports are given as magnitudes with directions indicated in Figs. 5 and 6.

vertical mixing but may also be a cross-section of the filamentation seen in the satellite image.

The next transect, T4, is a long section which appears to clip the edge of the STF at least once after leaving the warm side. This is consistent with the satellite image that shows a warm filament crossing the section. In fact, we altered course on this transect because it appeared we were crossing back onto the warm side of the front. We again had instrument problems at the end of this transect but it appears that we were well past the STF and on the cold side. Shallow CTDs were again used to fill in gaps. One interesting feature here is that while crossing into the filament we observed an offset between the surface expression of the STF and the deeper signature below the mixed layer. The onset of the STF in the SeaSoar record above the mixed layer occurs nearly 50 km before (km 1040) the STF based on the $T_{12}$ criterion below the mixed layer (km 1086). However, the maximum temperature and salinity occur nearly 50 km after the deeper maximum. It may be that the STF was oriented more obliquely to the transect in the mixed layer; this suggests that the two layers may have become decoupled at this point. The ADCP record supports this view as the velocity profiles are quite strongly sheared in the vertical along T3 and T4.

Heading back north on T5 we encountered biological fouling of the instrument between km 1480 and 1600. This lead to high frequency noise in the salinity record. Prior to this, however, we observed a high level of finestructure with horizontal scales on the order of a few kilometers and vertical scales often less than 10 m. Most of the structure is compensated which suggests that the observations are not artefacts

Table 2
Locations of significant front crossings based on the $T_{12}$ criterion and STF features mentioned in the text

| Season | Transect | Location (km) | Enter warm side (km) | Enter cold side (km) | Notes |
|---|---|---|---|---|---|
| Winter | T1 | 0–168 | | 127 | |
| | T2 | 168–546 | 314 | | |
| | T3 | 546–813 | | 720 | |
| | T4 | 813–1019 | | | |
| | T5 | 1019–1308 | 1050 | | |
| | T6 | 1308–1514 | | 1364 | |
| | T7 | 1514–1936 | 1638 | | |
| | T8 | 1936–2531 | | 2293 | Subsurface anomaly: 1960–1985 km |
| | T9 | 2531–2873 | 2824 | | |
| | T10 | 2873–3220 | | 2978 | |
| | T11 | 3220–3583 | | | |
| | T12 | 3583–3867 | | | Cold filament: 3785–3800 km |
| | T13 | 3867–4054 | | | Numerous cold intrusions |
| Summer | T1 | 0–260 | 189 | | Subsurface anomaly: 89–175 km |
| | T2 | 260–512 | | 300 | Subsurface anomaly: 309–340 km |
| | T3 | 512–828 | 761 | | |
| | T4 | 828–1264 | | 1132 | Warm filament: 1086–1131 km |
| | T5 | 1264–1759 | 1592 | | Biological fouling |
| | T6 | 1759–2143 | | 2071 | |
| | T7 | 2143–2562 | 2261 | 2492 | Warm filaments: 2261–2344 and 2416–2492 km |
| | T8 | 2562–2904 | 2734 | | Warm Filaments: 2734–2786 and 2785–2907 km |
| | T9 | 2904–3263 | | 2908 | Biological fouling |
| | T10 | 3263–3553 | 3425 | | Biological fouling |
| | T11 | 3553–3794 | | | Salinity anomaly: 3500–3600 km |

from the biological contamination. At the end of this transect we encountered what appears to be part of an eddy, the strong ADCP velocities and the domed density structure both support this interpretation. The satellite image also indicates a rather large 18 °C intrusion at the end of T5.

The satellite image shows that we crossed the STF several times during T6 and T7. During both transects we were running almost parallel to the STF which would account for the high density of fine structure. Towards the end of T6 we again encounter a large number of vertical features which are reminiscent of those observed at the end of T3. The two front crossing in T7 clearly correspond to the two filaments seen in the satellite image. In both sections, the fine structure is strongly compensated while the larger scale STF features are only moderately compensated and associated with strong ADCP velocities.

T8 runs southward along the axis of a large warm filament (Fig. 2). Before reaching the cold side of the front, we crossed the warm core of the filament at least twice. The most striking aspect of this transect is that the first crossing is almost completely density compensated while the second crossing is quite weakly compensated. The ADCP velocities for both crossings are consistent with a tightly curved filament with negative velocities on the inside of the curve and positive velocities on the outside.

Unfortunately, the salinity records for T9 are quite badly contaminated by biological fouling. The temperature record, however, indicates that, according to the $T_{12}$ criterion, we remained on the subpolar side of the STF for the whole transect. As during the winter cruise, we came up to the shelf and did not see the STF.

Unlike the winter cruise, we do eventually satisfy the $T_{12}$ criterion again south of this transect, but there is still some question of STF continuity between these two sets of observations. We again reach water characteristic of the subtropical side of the STF during T10, near km 3425. We appear to leave this water some 100 km later, the surface water becomes substantially cooler ($<14$ °C) even though the 12 °C

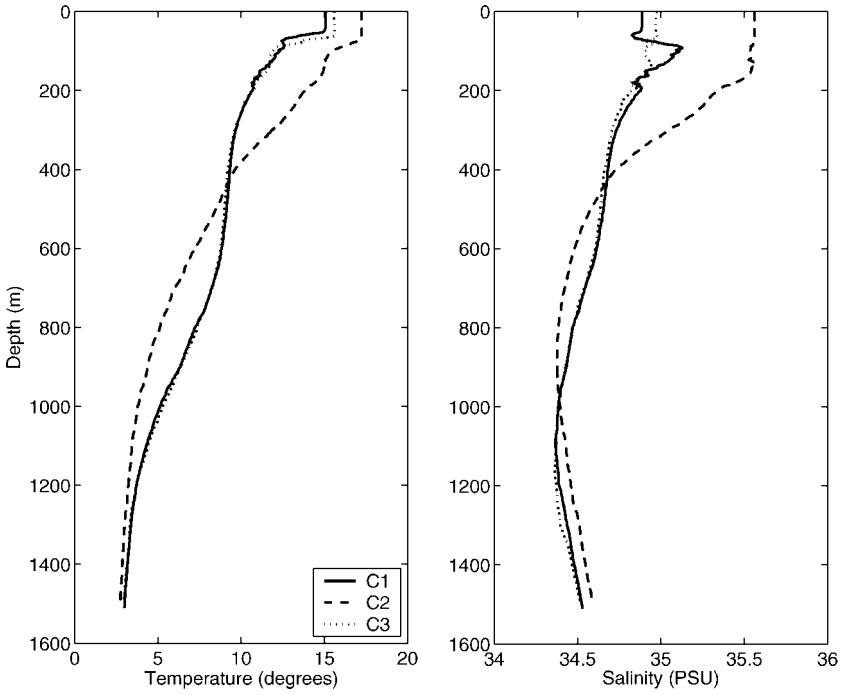


Fig. 9. 1500 m temperature and salinity profiles for the first three CTDs of the summer cruise, FR 02/98.

isotherm depth remains below 150 m. This may reflect a deeper mixed layer although we cannot rule out a decoupling of the mixed layer since there is a strong subsurface salinity structure that starts at 50 m and extends from km 3500 to 3600.

The last transect, T11, runs south of Tasmania and then north eastward towards Tasmania. We again see characteristics of the STF which are similar to the features of the first transect at the western edge of the study. In particular the 12 °C isotherm follows the $26.65\sigma_t$ isopycnal, although the SST is considerably cooler at this latitude.

## 4. Discussion

The observations made during the two cruises allow us to address three specific questions:

1. How is the existence of the STF related to local wind forcing within the SCZ?
2. Is the STF a continuous feature from the Indian Ocean to the Pacific Ocean?
3. How significant is the observed density compensation?

### *4.1. Wind forcing*

The STF exists as a band of enhanced horizontal temperature and salinity gradients within the SCZ. This suggests a process of frontogenesis with space scales smaller than the scales of the climate belts that determine the ocean-wide wind stress curl field. Large seasonal excursions of the STF, particularly in the Indian Ocean, point towards the local wind field as the dominate controlling factor, yet one key finding of the summer voyage is the existence of the STF at its normal location below the mixed layer. This indicates that the STF is not simply a response to local wind forcing, at least not during all seasons. It is possible that the detailed structure of the wind stress curl field produces a maximum in the meridional SST and SSS gradients during winter. This must somehow maintain the established density field through the summer when the formation of a shallow mixed layer decouples it from the wind stress curl.

One possible explanation is to assume a reasonably strong pressure gradient that can sustain the front in the absence of atmospherically induced frontogenesis. Running counter to this idea, however, are the observations that the geostrophic current is extremely small during summer (Table 1) and that horizontal density-gradients are weak due to density compensation.

Another possible explanation for how the STF can survive lengthy periods, isolated by the surface mixed layer from atmospheric forcing, may come from the density compensation itself. Rudnick and Ferrari (1999) make the point that density fronts tend to "slump" resulting in shear dispersion, whereas density compensated fronts, in the absence of a diffusive mechanism, tend to persist for long periods.

Although large-scale subsurface anomalies may be explained by geostrophically balanced advection beneath the mixed layer, another mechanism is needed to account for the many small-scale billows and inversions which are a particular feature of the summer voyage. One possibility is periodic wind forcing. The location of the STF on the poleward side of the SCZ places it on the southern edge of the atmospheric high pressure belt of the subtropics. This is the region where atmospheric frontal systems travel eastward, exposing the oceanic surface layer to strong winds with systematic changes in wind direction. These atmospheric fronts move the Ekman layer back and forth, creating eddies and shearing the upper mixed layer off from the underlying oceanic structure.

If the front is perfectly compensated, then advection of an Ekman layer cannot lead to convection by itself as the local static stability remains unaffected. However, two other mechanisms are possible: surface cooling due to sensible heat flux or double diffusion. If the Ekman layer is displaced poleward, warm salty water is moved over cooler fresher water creating the classic salt fingering scenario. Mixing in the surface layer, however, is too strong to allow salt-fingering to generate structures on the vertical scale seen in the transects. The sensible heat flux, on the other hand, is enhanced as warm water is moved poleward and convection is possible. Deepening of the mixed layer due to convection could leave remnants when the wind field reverses and the Ekman layer moves equatorward again. In the mixed layer the SST and SSS properties have changed as a result of the convection event. In this case, moving weather systems would produce large horizontal variability in the mixed layer and pockets of frozen convection just below the mixed layer.

The observations from this voyage provide some evidence for the proposed mechanism, particularly in the salinity field. The salinity is at best weakly affected by seasonal change so the horizontal salinity change associated with the STF usually reaches through the mixed layer. The salinity is therefore an ideal tracer for frozen convection events. Figs. 3 and 4 show that over hundreds of kilometers the interface between the mixed layer and the stratification below is marked by small parcels of water of lower salinity than its surroundings but similar to the salinity found on the subpolar side of the front. It is important to note, however, that these water parcels are not only found on the subtropical side but seem to exist on both sides of the front. In addition, although the front is compensated to a degree, in general the temperature has a stronger influence on the density field than the salinity. These observations, therefore, cannot completely exclude other possible formation mechanisms.

Another observation of significance is the clear correlation between the location of the STF below the mixed layer and the existence of SST fronts, at much higher temperatures than those associated with the STF, at the same location. It is difficult to imagine that a front in the mixed layer produced by the particularities of the local wind stress curl field always happens to be located where the 12 °C isotherm rises or falls across the 150 m depth level. This is especially true when you consider that in this region, during the summer, the 12 °C isotherm is not reached at all by local atmospheric processes. A more likely explanation appears to be that the lowered temperatures found at the surface whenever the 12 °C isotherm comes close to the mixed layer are the result of entrainment. The mixed layer temperature is the result of heat input from above and entrainment from below. Where the water below the mixed layer is relatively cold, as is the case on the subpolar side of the STF, the resulting mixed layer temperature can be expected to be lower than on the subtropical side where the underlying water is warmer.

### 4.2. Continuity of the STF

One of the initial questions during the cruise planning stage was whether the STF is continuous

between the Indian and Pacific Oceans. Belkin and Gordon (1996) reflect the general belief that it is; based on CTD and bottle data from historical meridional sections, they show the STF as a continuous feature along 39–40°S that bends southward as it approaches Tasmania and continues into the Tasman Sea along 47°S. While the data set used by the authors shows numerous STF crossings, between 37° and 40°S, in the western half of our survey region (115–135°E), only two STF observations near 45°S are reported between 135°E and Tasmania at 145°E. These observations are clearly insufficient to resolve issues of continuity and seasonal variation between 135° and 147°E, south of Tasmania, where data density increases somewhat and five observations of STF crossings are found between 45° and 47.5°S.

The combination of results from the summer and winter voyage allows a more definite statement on the location of the STF south of Australia. Assuming that the observations made in July/August and January/February 1998 are typical of winter and summer conditions, the situation can be described as follows:

*Winter*: During winter, the STF south of Australia is located near 38–39°S. It is not continuous between the Indian and Pacific Oceans but encounters strong westward flow south of Tasmania. It ends at the continental shelf west of Bass Strait near 40°S.

*Summer*: During summer, the temperature expression of the STF is covered by a 50–70-m-thick mixed layer but continues to exist below the mixed layer in the permanent thermocline. Its salinity expression extends through the mixed layer to the surface. The location of the STF does not change much during the year—the data from the summer voyage show that it is found at 38–39°S and produces large filaments as it approaches Bass Strait. These filaments can push southward beyond 40°S. Unlike the winter cruise, we did not profile all the way onto the shelf so it is not possible to categorically rule out STF continuity. In fact, the STF is observed again in the last transect (T11) south of Tasmania. However, eddies are likely to be spawned by the STF in the Tasman Sea, where it is found at 43–44°S (Szymanska and Tomczak, 1994) and the STF seen in this transect may be an expression of the STF of the Pacific Ocean.

Rintoul and Bullister (1999) and Rintoul et al. (1997) report observations of the STF south of Tasmania. The data sets used by Rintoul et al. (1997) show the front with temperatures and salinity that correspond to the frontal identifiers listed by Belkin and Gordon (1996) and used in this paper. Most of these data sets are summer ones, support for the presence of the STF south of Tasmania during other seasons comes from one data set obtained during autumn (March 1993) and used by Rintoul et al. (1997), and from data obtained during spring (September/October 1991) and used by Rintoul and Bullister (1999). Our summer observations also indicate the presence of the STF south of Tasmania during summer. But observations of the STF south of Tasmania are not sufficient to demonstrate continuity further to the west, more observations between 135° and 145°E will be needed to clarify the issue of continuity or discontinuity and its seasonal dependence. Another possibility that has been raised is that the STF may have multiple branches in this region. It is known, for example, that the STF has multiple branches in other regions such as the Indian Ocean and South Atlantic (Belkin and Gordon, 1996). This raises the question of whether we have surveyed a northern, warmer branch of the STF that was discontinuous while a southern, cooler branch may have been continuous. Because of the deep mixed layer, the winter SST image (Fig. 1) is a better predictor of sub-surface structure than the summer image. In the winter SST image the gradients south of our survey are quite weak so if there is a southern branch to the STF it would have to be south of 45°S. Looking at the summer SST image (Fig. 2) it is possible to make a case that strong SST gradients exist south of the region we surveyed, but the image shows no obvious connection between these gradients and the reestablishment of the STF south of Tasmania. In either case we do not have sufficient data from these surveys to speculate further on possible branching of the STF.

### 4.3. Density compensation

Any discussion of density compensation should keep in mind that density compensation is a natural condition of the upper kilometer of the ocean. Central Water (the water mass of the oceanic thermocline) is characterized by a temperature–salinity relationship

in which both properties decrease with depth. The variation of salinity therefore always compensates the effect of temperature variations on density to some degree (i.e. $0°>T_H>90°$), and the same is true for the meridional variations of SST and SSS in the subtropics. It is the degree of compensation that distinguishes the STF, specifically the degree of compensation below the mixed layer.

Recent studies suggest that strong compensation in the mixed layer may be relatively common (Rudnick and Ferrari, 1999; Rintoul and Bullister, 1999; Rintoul et al., 1997). Below the mixed layer, however, we should compare the situation in the STF south of Australia to other frontal profiles. For example, Fig. 10 shows the horizontal Turner angle $T_H$ as a continuous function of depth within the Azores Front from three separate SeaSoar tracks taken during the late spring and winter (Rudnick and Luyten, 1996). We note that below the mixed layer, $T_H$ is always near or above 60°. In this case, the Azores Front resembles the more usual situation where $T_H=63.4°$, corresponding to the density ratio $R_\rho=2$.

To predict the degree of density compensation within the mixed layer, there are essentially two models: Stommel (1993) proposed a mixed layer regulator that predicts $T_H=63.4°$, while Young (1994) uses a shear dispersion model that predicts $T_H=45°$ ($R_\rho=1$). The Stommel model was motivated by observations that over large scales the average mixed layer horizontal density ratio approaches 2. Young's model, on the other hand, is applicable to smaller horizontal scales such as those involving oceanic fronts (Chen and Young, 1995). Within the mixed layer, the STF south of Australia behaves closer to the predictions of the model proposed by Young.

One possible explanation for the high compensation below the mixed layer may be due to the seasonal variability of the mixed layer depth and the persistence of density compensated fronts in general. Dur-

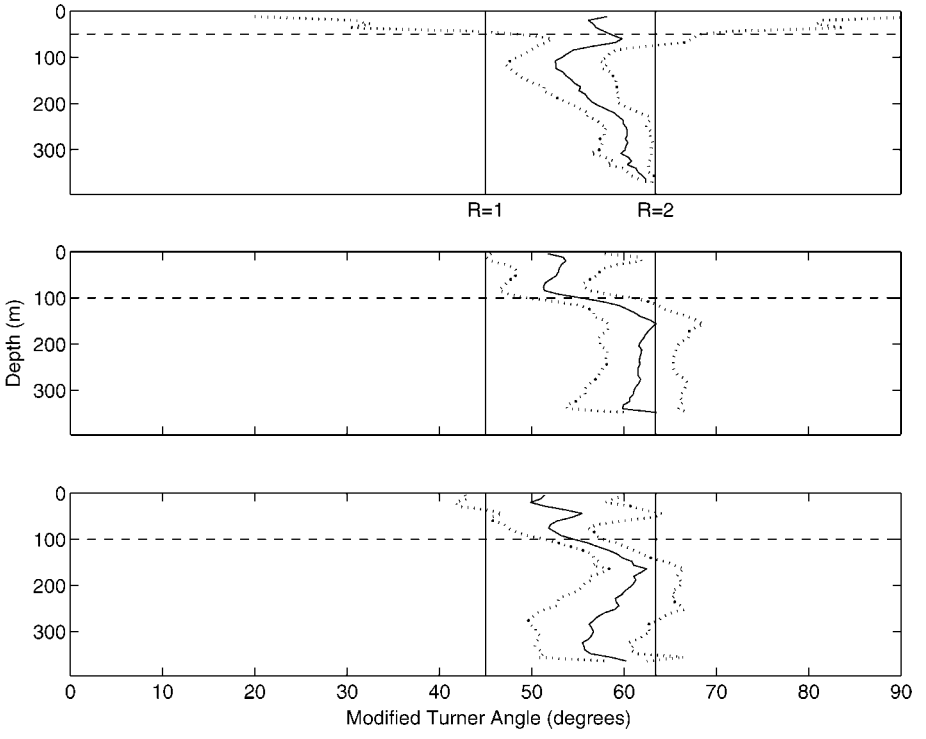


Fig. 10. The modified Turner angle (see text) as a function of depth for the Azores Front surveys. Dotted lines indicate error estimate described in text, horizontal dashed lines indicate the approximate mixed layer depth. Data are from Rudnick and Luyten (1996).

ing the first half of the winter cruise, the mixed layer appears to be close to 150 m deep while the mixed layer depth frequently exceeds 300 m during the last half of the cruise as we move further east and south. Two transects at the end of the winter cruise, T10 and T11, show a mixed layer depth close to 300 m. The Turner angle in Fig. 7 indicates near perfect density compensation at 250 m at the end of the winter cruise and this is almost certainly due to the depth of the mixed layer.

During the summer, the mixed layer is only about 50 m deep and it is possible that the high compensation below the mixed layer observed during the summer is due to the SeaSoar profiling structures actually formed in the winter mixed layer. This mechanism is supported by the previously stated fact that density compensated fronts can persist once formed and by our own observations of frontal features below the mixed layer during the summer.

While we cannot rule out this mechanism, it is important to note that the summer Turner angle is measured at 180 m while the winter mixed layer depth for most of the cruise was around 150 m. Since the winter and summer cruises occurred toward the end of their respective season, both mixed layers depths should have been close to their seasonal extremes. The layer below the summer mixed layer is clearly subject to some disturbance as evidenced by the variety of sub-mixed layer features in the profiles. It seems unlikely that density compensation could persist for a season or more in the presence of such disturbances.

## 5. Conclusion

It is clear from these tentative remarks that the dynamics of the STF south of Australia will require a detailed and comprehensive study. Such a study will have to identify the processes leading to frontogenesis, while taking into account the effect of density compensation on the regional scale and its effect on the pressure gradient, and small scale mixing processes. The study should account for the STF's observed persistence during the summer when it is masked by a shallow mixed layer with which it interacts, as well as the apparent collapse of the STF, west of Tasmania, into numerous eddies and filaments. The question of frontal stability and persistence in the presence of filamentation, interleaving and double diffusion is the subject of the ongoing work.

## Acknowledgements

We would like to thank the officers and crew of the R/V *Franklin*, and the technical support of CSIRO without which this SeaSoar project would not have been possible. We would like to particularly thank Stuart Godfrey, Steve Rintoul and two other anonymous reviewers for their helpful comments.

## References

Belkin, I.M., Gordon, A.L., 1996. Southern Ocean fronts from the Greenwich meridian to Tasmania. Journal of Geophysical Research 101, 3675–3696.

Chen, L., Young, W.R., 1995. Density compensated thermohaline gradients and diapycnal fluxes in the mixed layer. Journal of Physical Oceanography 25, 3064–3075.

Deacon, G.E.R., 1960. The southern cold temperate zone. Proceedings of the Royal Society London, Series B 152, 441–447.

Herzfeld, M., 1997. The annual cycle of sea surface temperature in the Great Australian Bight. Progress of Oceanography 39, 1–27.

Lennon, G.W., Bowers, D.G., Nuñes, R.A., Scott, B.D., Ali, M., Boyle, J., Wenju, C., Herzfeld, M., Johansson, G., Nield, S., Petrusevics, P., Suskin, A.A., Wijffels, S.E.A., 1987. Gravity currents and the release of salt from an inverse estuary. Nature 327, 695–697.

Nagata, Y., Michida, Y., Umimura, Y., 1988. Variation of positions and structures of the oceanic fronts in the Indian Ocean sector of the Southern Ocean in the period from 1965 to 1987. In: Sahrhage, D. (Ed.), Antarctic Ocean and Resources Variability. Springer-Verlag, New York, pp. 92–98.

Orsi, A.H., Nowlin Jr., W.D., Whitworth III, T., 1993. On the circulation and stratification of the Weddell Gyre. Deep-Sea Research 42, 169–203.

Rintoul, S.R., Bullister, J.L., 1999. A late winter hydrographic section from Tasmania to Antarctica. Deep-Sea Research 46, 1417–1454.

Rintoul, S.R., Donguy, J.R., Roemmich, D.H., 1997. Seasonal evolution of upper ocean thermal structure between Tasmania and Antarctica. Deep-Sea Research I 44, 1185–1202.

Rudnick, D.L., Ferrari, R., 1999. Compensation of horizontal temperature and salinity gradients in the ocean mixed layer. Science 283, 526–529.

Rudnick, D.L., Luyten, J.R., 1996. Intensive surveys of the Azores Front: 1. Tracers and dynamics. Journal of Geophysical Research 101, 923–939.

Schmitt, R.W., 1999. Spice and the demon. Science 283, 498–499.

Schodlok, M., Tomczak, M., 1997. The circulation south of Aus-

tralia derived from an inverse model. Geophysical Research Letters 24, 2781–2784.

Schodlok, M.P., Tomczak, M., White, N., 1997. Deep sections through the South Australian basin and across the Australian–Antarctic discordance. Geophysical Research Letters 24, 2785–2788.

SCOR Working Group 69, 1988. Small-scale turbulence and mixing in the ocean: a glossary. In: Nihoul, J.C.J., Jamart, B.M. (Eds.), 1988. Small-Scale Turbulence and Mixing in the Ocean. Elsevier, Amsterdam, pp. 3–10.

Stommel, H.M., 1993. A conjectural regulating mechanism for determining the thermohaline structure of the oceanic mixed layer. Journal of Physical Oceanography 23, 142–148.

Stramma, L., 1992. The south Indian Ocean current. Journal of Physical Oceanography 22, 421–430.

Stramma, L., Peterson, R.G., 1990. The South Atlantic Current. Journal of Physical Oceanography 20, 846–859.

Stramma, L., Peterson, R.G., Tomczak, M., 1995. The South Pacific Current. Journal of Physical Oceanography 25, 77–91.

Szymanska, K., Tomczak, M., 1994. Subduction of Central Water near the Subtropical Front in the northern Tasman Sea. Deep-Sea Research 41, 1373–1386.

Tomczak, M., Godfrey, J.S., 1994. Regional Oceanography: An Introduction. Pergamon, New York, 422 pp.

Young, W.R., 1994. The subinertial mixed layer approximation. Journal of Physical Oceanography 24, 1812–1826.